



Royal Netherlands
Meteorological Institute
*Ministry of Infrastructure
and Water Management*

Advice on the computation of peak-ground-velocity confidence regions for the Zuidlaren 23-12-2016 event

E. Ruigrok, B. Dost

De Bilt, 2020 | Technical report; TR-382

Advice on the computation of peak-ground-velocity confidence regions for the Zuidlaren 23-12-2016 event

KNMI, R&D Seismology and Acoustics

December 12, 2019

Summary

On request by the Technical Committee on ground movement (Tcbb), a study was carried out to define the region affected by induced earthquakes related to gas exploitation from gas fields outside the Groningen area. This request is based on advise that the Tcbb formulated in 2019, on a national approach for handling damage due to mining. Since there is no generic ground-motion model for gas fields outside the Groningen area, assumptions should be made with respect to the selection of the best model for the region. Most important is the build-up of the overburden of the gas field, combined with the availability of recorded acceleration data in the vicinity of the gas field. The 2016 induced earthquake near Zuidlaren was used to test the proposed procedure and results are presented in terms of contour plots of expected Peak Ground Velocity (PGV) contours for 1 mm/s until the maximum level, with a 1, 10 and 50% probability of exceedance.

1 Introduction

KNMI was asked by the Technical Committee on ground movement (Technische Commissie bodem beweging, Tcbb) to compute maximum ground velocities at the earth's surface for a recent induced seismic event near the town of Zuidlaren, south of Groningen. This event is connected to the Annerveen gas field. Specifically the request refers to the Peak Ground Velocity (PGV) values for the maximum values of the horizontal components after rotation and for a 1%, 10% and 50% probability of exceedance for PGV levels of 1 mm/s until the maximum level, with steps of 1 mm/s.

Structures are mostly sensitive to seismic waves in the frequency range in which these structures resonate. The PGV is a proxy for the ground movement in this frequency range and is widely used to assess potential earthquake damage. Also the Dutch guideline on assessing building damage (*Jonker et al.*, 2017) is expressed in terms of PGV. This directive lists PGV threshold values for buildings that yield a 1% chance of inflicting damage. These PGV values range from 3 mm/s for sensitive brickwork, to 5 mm/s for conventional brickwork and to 20 mm/s for concrete and wooden structures. For repeated occurrence, lower PGVs could inflict damage.

For each threshold PGV, Tcbb proposes to define a region around an earthquake that has a 99% certainty that all PGVs of that level that actually materialized are within this region (*report TCBB*, 2019). This region could quite well be modeled if detailed source parameters were known, like hypocenter, magnitude, moment tensor and rupture direction. Moreover, a detailed subsurface model needs to be available to forward model waves propagating from

the source to just below the sites. And, local site conditions describing the local amplifications of waves, need to be a-priori known and incorporated.

For events in Groningen, a detailed ground-motion model has been derived (*Bommer et al.*, 2017) and a dense network of surface recordings is available (*Dost et al.*, 2017). This allows computation of shake maps, which show the ground movement at the Earth's surface. These can be used, among others, for damage assessment. In addition, a simplified version of the ground-motion model for Groningen was developed, namely a fully empirical PGV model, only valid for a limited magnitude range (M 1.8-3.6) (*Bommer et al.*, 2019).

For events outside Groningen, the measuring network is more sparse and site conditions are not well known. In this case, one needs to resort to a more generic ground-motion-prediction equation (GMPE) with an uncertainty, that incorporates the large differences in, among others, site conditions.

A GMPE is a function that describes the decay in amplitude as function of distance and magnitude. Sometimes the focal depth is added as a third variable. A large suite of GMPEs has been derived for various settings. Three empirical GMPEs exist that have been derived for seismicity with low magnitudes (<5) and shallow focal depths (<10 km) and that have been calibrated, purely or partly, with Dutch data. The first such model is described in *Dost et al.* (2004) in which seismicity outside Groningen is used for calibration. The second model (*Douglas et al.*, 2013) uses partly the same Dutch data as in *Dost et al.* (2004), but adds to this data from geothermal areas in Europe. The third model has been calibrated with data from Groningen only (*Bommer et al.*, 2019). The models are averages over many different sites and earthquakes. These variation add to the uncertainty in the models, which has been quantified in all three of them.

Different studies (e.g., *Douglas et al.*, 2013) have shown that the nature of the seismicity, whether induced or natural, is not relevant for the observed PGVs. What is relevant is the subsurface setting. In the Netherlands, there is mainly a division in two reservoir settings. One with a salt layer in the overburden, and one without. This salt layer has much higher elastic impedance than the underlying rock and therefore reflects part of the seismic wavefield induced at reservoir level, leading to a smaller proportion of the wavefield reaching the Earth's surface (*Kraaijpoel and Dost*, 2013). In the other reservoir setting, such a high-impedance layer does not exist in the overburden. As a consequence, higher PGVs will be observed at the Earth's surface, for the same earthquake magnitude. Mixing data from the two different settings would lead to very large spread in recorded PGVs (for the same magnitude, distance and focal depth). Hence, in the following we will propose to disentangle data from these two settings.

In this report, we evaluate which GMPE(s) would be suitable for events outside Groningen. We choose a GMPE for the Zuidlaren event on 23-12-2016:14:29:49.5, which is an earthquake that happened in the Annerveen gas field, which is just south of the Groningen field. For this event, we compute the PGV threshold regions.

2 Existing GMPEs

2.1 Dost

The Dost GMPE has been published in *Dost et al.* (2004). It is based on an attenuation relation derived for the north of the Netherlands, which has been derived for the purpose of magnitude computation with geophones installed at depth. This attenuation relation has been scaled with recordings at the Earth's surface at three source regions in or near the

Netherlands: Voerendaal, Alsdorf and Roswinkel. All three regions have seismicity at depth without an overlaying salt layer. These source regions have different depths and hence a depth dependency has been introduced. The relation reads

$$\log(PGV) = -1.53 + 0.74M - 0.00139r - 1.33 \log(r), \quad (1)$$

where r is the hypocentral (source-to-site) distance, M is the local magnitude and PGV is the geometric mean over both horizontal components.

In this model, no saturation has been built in for higher magnitudes. The model was obtained from earthquakes with magnitudes between 0.8 and 4.9. Most of the used strong motion recordings are from within 5 km distance. However, the underlying attenuation relation is from a much wider epicentral distance range. The total uncertainty σ reads 0.33, expressed in $\log(PGV)$.

2.2 Douglas

Douglas et al. (2013) derived a GMPE specifically for geothermal areas. Their model is based on data from 6 source areas. Besides from 4 geothermal areas, data is included from natural seismicity (Voerendaal) and from gas extraction (Roswinkel). They used data with focal depths down to about 10 km and hypocentral distances until 50 km. They derived a model including and excluding site effect. Their mean PGV model including (average) site effects reads

$$\ln(PGV) = -10.367 + 2.018M_w - 1.124 \ln(\sqrt{r^2 + 2.129^2}) - 0.046r, \quad (2)$$

where \ln is the natural logarithm, M_w is the moment magnitude, r the hypocentral distance and PGV is the peak ground velocity obtained by taking the geometric mean over both horizontal components.

Uncertainties in the model are large, probably due to combining data from different type of sources and largely varying subsurface and site conditions. The within-event uncertainty ϕ , the between-event uncertainty τ and total uncertainty σ are 1.11, 0.745 and 1.958, respectively. These are uncertainties expressed in $\ln(PGV)$.

2.3 Bommer

The Bommer model (*Bommer et al.*, 2019) is parameterized as

$$\ln(PGV) = c_1 + c_2M + g(R^*), \quad (3)$$

where M is the local magnitude, $g(R^*)$ is a function that describes the geometrical spreading and R^* is defined as follows

$$R^* = \sqrt{R^2 + [e^{0.4233M - 0.6083}]^2}, \quad (4)$$

where R is the epicentral distance. Equation 4 expresses the magnitude-dependent distance saturation term. Further details on the geometrical spreading term and the values for the coefficients c , can be found in the reference.

The GMPE has been derived for three different definitions of PGV , leading to different numerical values for c in equation 3. Here, to be consistent with the other two models, we use the model for geometric mean. This model gives smaller values of PGV than with the other two definitions of PGV, which are PGVmax (maximum recorded ground velocity at one of the two horizontal components) and PGVrot (maximum ground velocity after rotating the horizontal components such that a maximum value in the horizontal plane is reached).

The Bommer model has an empirical base between $M=1.8$ and $M=3.6$ and for distances up till 35 km. Note that the GMPE has been derived with Groningen data only. Hence, for a reservoir below a thick layer of salt at around 3 km depth. In its current form, this relation is only to be used in cases where a similar setting is encountered as in Groningen. Uncertainties in the model are split up into within-event uncertainty ϕ and between-event uncertainty τ , which are 0.48205 and 0.25128, respectively. This yields a total uncertainty $\sigma = \sqrt{\phi^2 + \tau^2}$ of 0.54361. The uncertainties are expressed in $\ln(PGV)$.

3 GMPE for Zuidlaren

In this section the most suitable GMPE is selected, from the three GMPEs introduced in the previous section. Afterwards, the source term and the confidence regions are computed. The intersection of the boundaries of the confidence zones and the PGV thresholds yield the radii that form the basis for obtaining the PGV threshold regions, which will be printed in Section 5, after first finding the epicentral uncertainty in Section 4.

3.1 GMPE selection

The Zuidlaren event was nucleated in the Annerveen reservoir, which is located just south of the Groningen gas field. The subsurface setting is similar to the Groningen field. The reservoir is a Rotliegend sandstone sealed by a thick layer of salt from the Zechstein formation. Hence, it is likely that the GMPE model that was constrained with Groningen data (Section 2.3) is most appropriate for this event.

Both the models and the measurements are expressed in terms of geometric means over both horizontal components. In *Dost et al.* (2018) it is shown that moment magnitude and local magnitude are equal (for Groningen seismicity) for magnitudes larger than 2.0. This makes it straightforward to include the Douglas model, which is expressed in moment magnitude.

Figure 1 shows the measured PGVs for the Zuidlaren event in comparison with the three GMPEs for a magnitude of 2.4 and a focal depth of 3 km. The measured PGV values are from the Groningen and Norg seismic networks. Both networks are described in *Dost et al.* (2017). On the Earth's surface, there is no seismic recording within the first 10 kilometers from the event. The recorded PGV values are below the Dost model, are mostly above the Douglas model and are, on average, quite well described by the Bommer model.

Since many PGV recordings are available for the Zuidlaren event, the different models can be shifted up and down to fit better data. By doing so, effectively the event term is estimated. A quite good fit with the data could be obtained if the Dost model was shifted down. The Douglas model would give a slightly worse fit, as its attenuation with distance is stronger than the data suggests. The Bommer model has, beyond 6.32 km, almost the same attenuation as the Dost model. Only a tiny shift would be needed to obtain an optimal fit to the data points.

Figure 2 shows the measured PGVs for the Froombosch event. This event had the same magnitude as the Zuidlaren event, but a better collection of near-field recordings. It shows that PGVs attenuate strongly over the first 5 km or so. The Dost model shows relatively modest attenuation within the first 5 km. The same is the case for the Douglas model. The Bommer model does show a large attenuation over the first 5 km, which is quite consistent with the Froombosch data points.

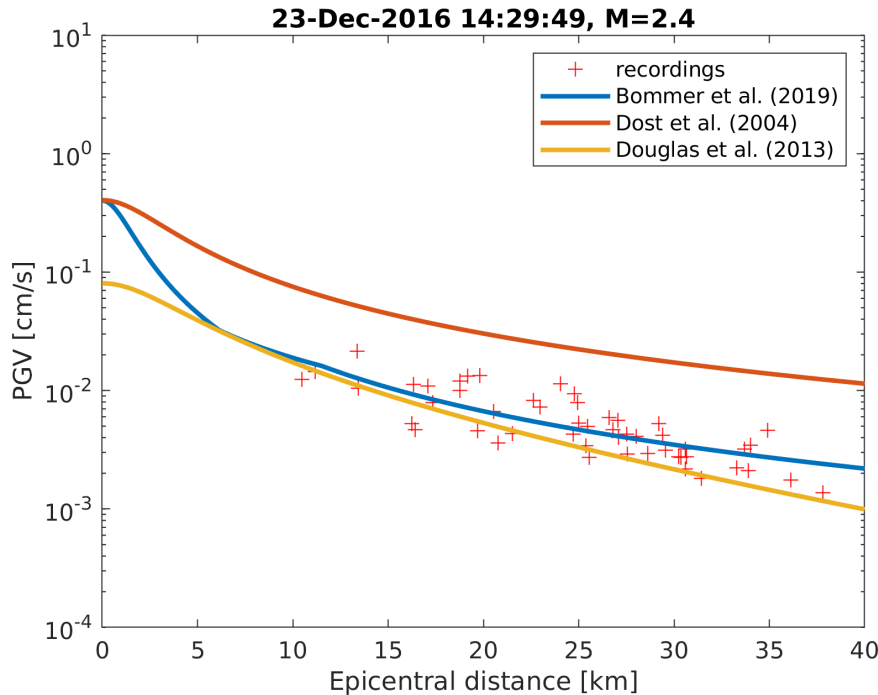


Figure 1: Mean GMPEs in comparison with PGV recordings for the Zuidlaren event.

The attenuation in the Bommer model has been constrained with a database of 1724 PGV recordings over Groningen, well sampling the distance range between 0 and 35 km. Since the subsurface setting for the Annerveen gas field is similar to the Groningen field, and the measured PGV values indeed show a good match with the Bommer model, we select this model. It could be that for other settings, without a salt layer in the overburden, the Dost or Douglas model is more descriptive.

3.2 Radii computation

For the Zuidlaren event we concluded that the Bommer empirical GMPE is the most suitable model to use. Since sufficient data is available, the mean GMPE is shifted such that residual with the data is minimized. By doing so, effectively the source term is estimated. This source term is descriptive for, e.g., the specific stress drop that occurred. For the Zuidlaren event, this source term, expressed in \ln , is 0.030. This corresponds to a tiny upward shift of the mean Bommer model, which is obtained by adding this event term to equation 3.

After the shifting, the within-event variability is used to compute the confidence regions. This variability has been quantified in *Bommer et al. (2019)* using the Groningen dataset, which has a large variability in site conditions (*Kruiver et al., 2017; Van Ginkel et al., 2019*). A similar variability is likely for other sites in the Netherlands and hence values at their Table 3.2 are used. This yields the confidence region as plotted in Figure 3. The intersections of the P99 line with the 2, 3 and 5 mm/s PGV thresholds yield radii of 4.1, 3.1 and 2.1 km, respectively. Using the P90 instead reduces the radii to 2.9, 2.1 and 1.2 km. With P50 (the mean model after event-term correction) the radii further reduce to 1.8, 1.0 and 0 km.

Following the request by the Tcbb, we use in the following the PGVrot model and also PGVrot distilled from the recordings. For this model, a least-squares fit with the PGVrot

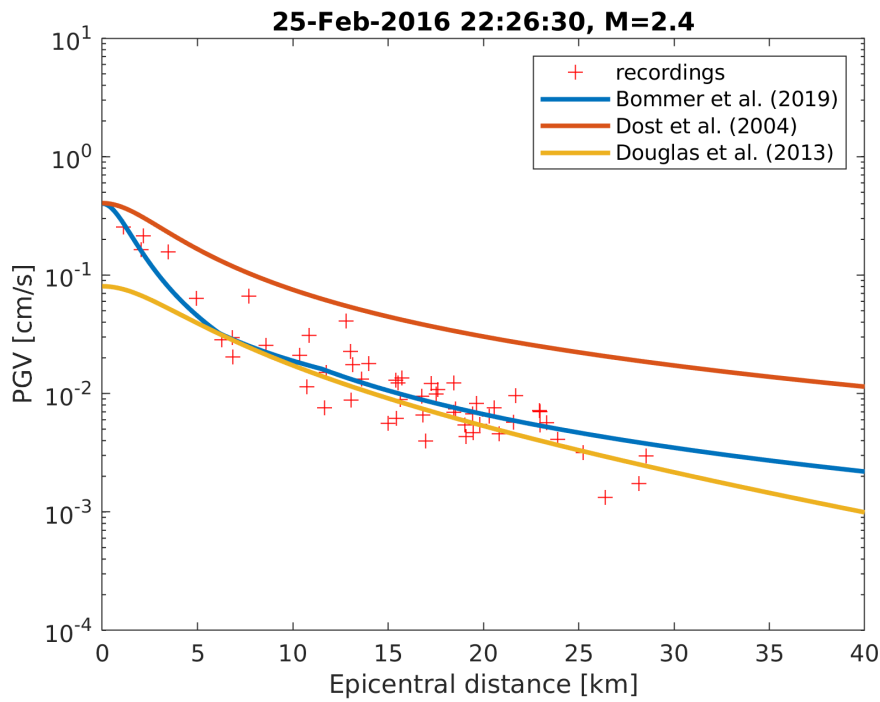


Figure 2: Mean GMPEs in comparison with PGV recordings for the Froombosch event.

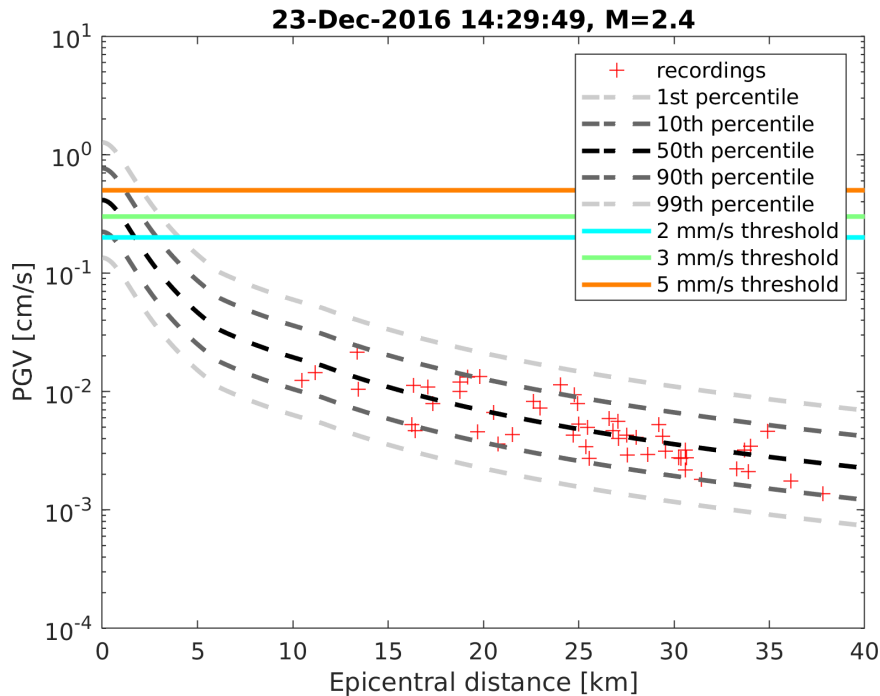


Figure 3: Bommer GMPE expressed in PGV_{geo} , confidence regions for that model (dashed lines), PGV thresholds (coloured lines) and measured PGV_{geo} values for the Zuidlaren event (red crosses).

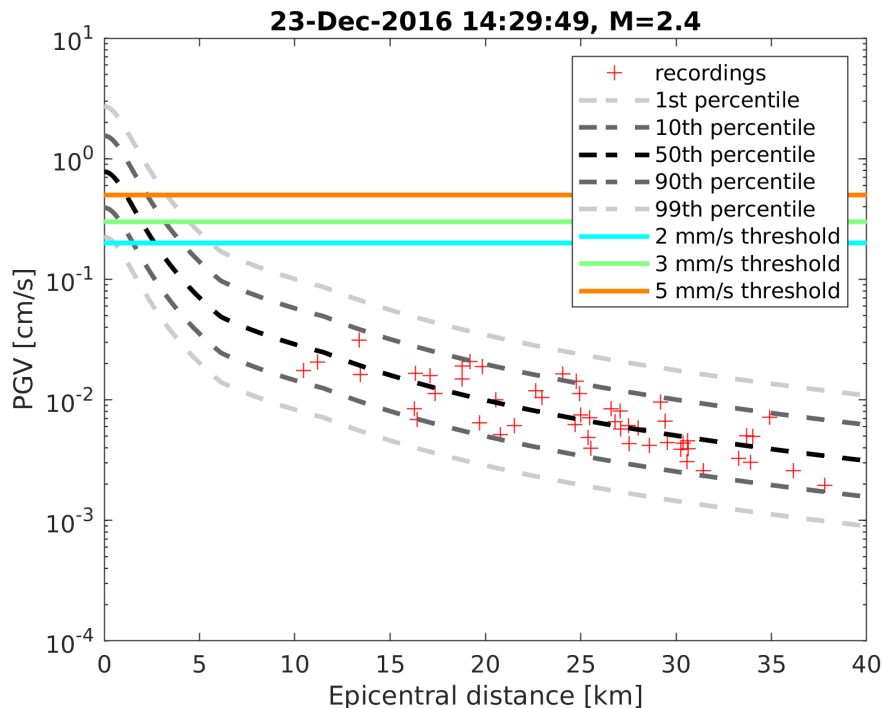


Figure 4: Bommer GMPE expressed in PGVrot, confidence regions for that model (dashed lines), PGV thresholds (coloured lines) and measured PGVrot values for the Zuidlaren event (red crosses).

data yields an event term of 0.14. After shifting the Bommer PGVrot mean model with this event term, the event specific P50 is obtained for the Zuidlaren event. For computing the P90 and P99 the within-event variability is used, which is 0.53613 for the PGVrot model. Figure 4 shows the resulting model and data points. The intersections of the P99 line with the 2, 3 and 5 mm/s PGV thresholds yield radii of 5.6, 4.5 and 3.3 km, respectively. Using the P90 instead reduces the radii to 4.1, 3.2 and 2.3 km. With P50 the radii further reduce to 2.7, 2.0 and 1.2 km.

4 Location

The Zuidlaren event on 23-12-2016:14:29:49.5 was detected by the KNMI network (KNMI, 1993) and located near-real time with the Hypocenter method (Lienert *et al.*, 1986). This fast solution uses an average 1D model for the north of the Netherlands (Kraaijpoel and Dost, 2013). Here the epicenter is improved by using a best-fitting traveltimes versus distance model based on a database of local P-wave traveltimes picks. This data-driven model naturally incorporates actual underburden velocities and only well pickable phase arrivals. An error estimate is derived from the spread in picking times from the best-fitting model. This error incorporates both the local variations of the velocity field as well as picking errors. These errors are propagated further into an epicentral probability density function (PDF). This results into an updated epicenter and its 95% confidence region. For post-2014 events within the Groningen network, also an updated hypocenter solution is available (Spetzler *et al.*, 2018).

Fig. 5 shows the seismic sensors where manual P-wave picks are available for this event. A

grid search is done for a region around the Hypocenter solution, as indicated by the red box in Fig. 5. In the first step, equal differential time (EDT, *Zhou, 1994*) residuals are computed. That is, for each grid point and for each station combination, the traveltime differences are forward modelled and tabulated. From these values, the observed traveltime differences are subtracted to obtain the EDT residuals. In the second step, the PDF (*Tarantola, 2005*) is derived from the EDT residuals, using a L1 norm. Fig. 6 shows the 95% confidence area of the resulting PDF¹. The location with the maximum probability is assigned to be the new epicenter.

In the following the relevant parameters are listed. The new epicenter is listed both in wgs84 and in the Dutch national triangulation system (RD). Also a gridded version of the 95% confidence contour of the PDF, and its major and minor axes, can be found.

Epicenter in wgs84 [deg]: 6.710, 53.068

Epicenter in RD [m]: 243680, 565360

PDF major axis [m]: 1629

PDF minor axis [m]: 946

Orientation of the PDF ellipse [deg]: 2.6

95% confidence contour RDx [m]: 243593, 243640, 243720, 243760, 243840, 243880, 243920, 243960, 243998, 244023, 244044, 244080, 244097, 244120, 244132, 244149, 244160, 244164, 244170, 244171, 244166, 244160, 244151, 244134, 244120, 244096, 244078, 244040, 244012, 243981, 243943, 243893, 243840, 243800, 243720, 243640, 243600, 243551, 243498, 243457, 243423, 243394, 243360, 243327, 243310, 243282, 243269, 243250, 243240, 243231, 243223, 243221, 243224, 243232, 243240, 243252, 243274, 243287, 243320, 243339, 243363, 243400, 243440, 243480, 243520, 243593

95% confidence contour RDy [m]: 564560, 564549, 564550, 564561, 564598, 564626, 564663, 564708, 564760, 564800, 564840, 564920, 564960, 565038, 565080, 565160, 565240, 565280, 565360, 565440, 565520, 565567, 565640, 565720, 565765, 565840, 565880, 565955, 566000, 566040, 566080, 566120, 566150, 566164, 566176, 566162, 566148, 566120, 566080, 566040, 566000, 565960, 565904, 565840, 565800, 565720, 565680, 565600, 565539, 565480, 565400, 565320, 565240, 565160, 565113, 565040, 564960, 564920, 564841, 564800, 564760, 564705, 564658, 564621, 564593, 564560

The underlying waveform data used in the above analysis is publicly available and can be obtained through

a GUI: <http://rdsa.knmi.nl/dataportal/>

FDSN webservices: <http://rdsa.knmi.nl/fdsnws/dataselect/1/>

5 PGV threshold regions

The Bommer GMPE has been derived for earthquakes in Groningen, with their inherent uncertainty in location. Events outside the Groningen area would in general have a larger epicentral uncertainty, due to a sparser seismic network. This additional uncertainty would need to be taken into account when computing the contours that bound the PGV threshold regions. For the Zuidlaren event we do not add an additional epicentral uncertainty.

¹Note that a smaller PDF would be obtained if also S-wave time differences and P-S delay times were included. For this purpose, the S-wave velocity model needs to be calibrated. This is work in progress.

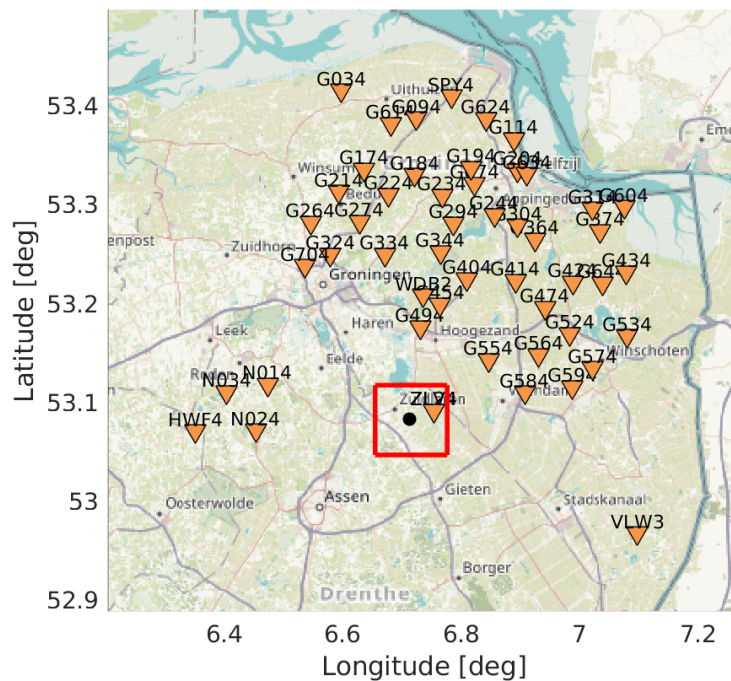


Figure 5: Overview map with locations of stations (yellow triangles) where P-wave onsets were picked, the fast Hypocenter solution (black dot) and the boundary line of the area in which a grid search is done (red box). Background map is from www.openstreetmap.org.

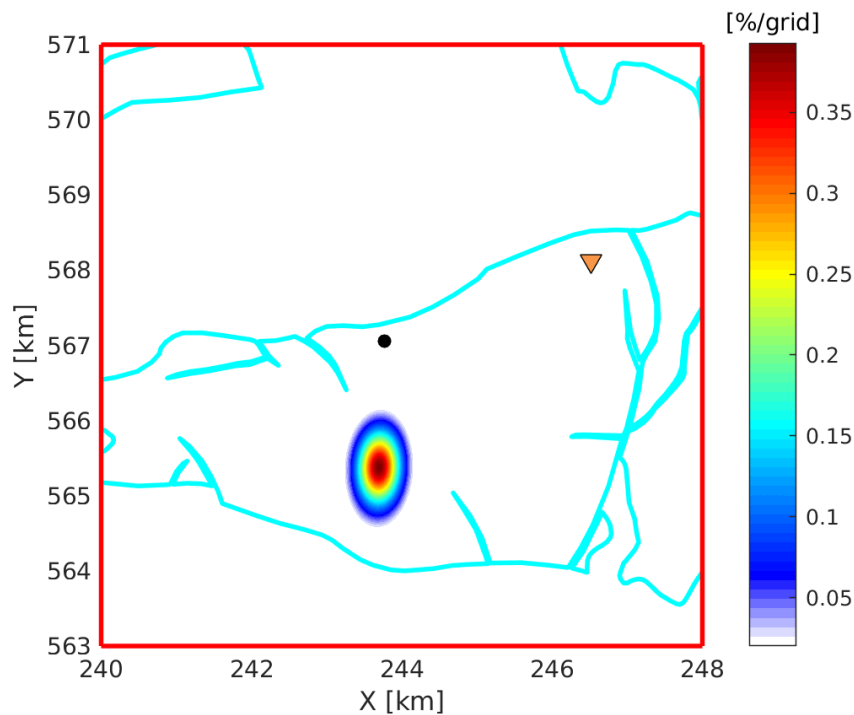


Figure 6: Map showing contours of gas fields (blue lines), the fast Hypocenter solution (black dot) and the epicentral probability density function (PDF) using time-differences and an optimized model. The 95% confidence area of the PDF is shown, with probabilities expressed in percentage per grid point.

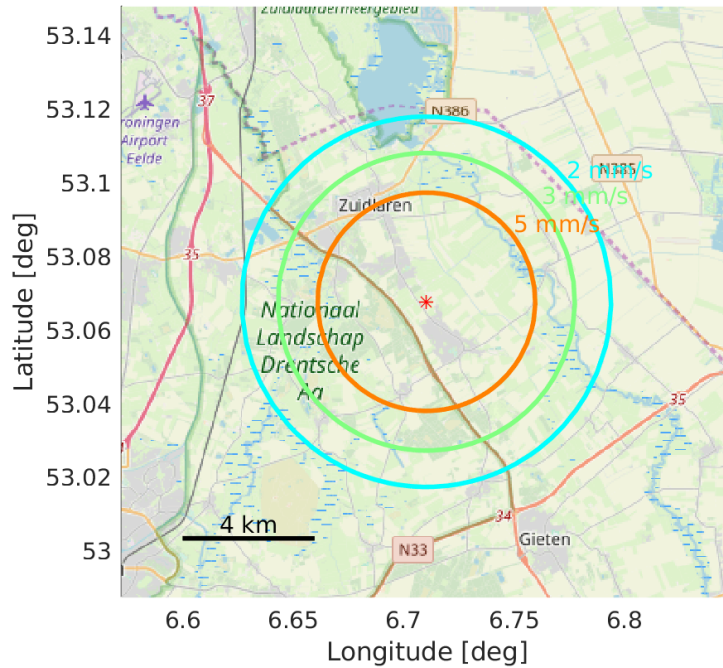


Figure 7: Circles showing the bounding lines of the 2, 3 and 5 mm/s PGV threshold regions for the P99 model, and the updated epicenter (red star).

The updated epicenter (Section 4) together with the computed radii for the P99, P90 and P50 models (Section 3.2) together define the PGV threshold regions. On Figure 7 the bounding lines for P99 are shown, for 2, 3 and 5 mm/s. Similarly, Figures 8 and 9 show the threshold regions for the P90 and P50 models, respectively.

In this report, only contours for 2, 3 and 5 mm/s are plotted. However, the complete range of radii is computed, from 1 mm/s to the maximum integer PGV expressed in mm/s. The corresponding contours expressed in wgs84 values are stored as kml files and are attached to this report.

Discussion and Conclusions

In the preceding we determined PGV threshold regions for an event outside of Groningen. For this testcase we used the Zuidlaren $M=2.4$ event.

The updated epicenter shows a large shift (1.7 km) to the south with respect to the fast solution that was obtained in the operational workflow. The underlying reason is that in this fast solution, also travel-time picks in Twente were used, whereas the used velocity model is not a good representation for the average subsurface between Zuidlaren and Twente. Removing these picks led to the shifting of the epicenter and a reduced uncertainty. After the occurrence of this event, the operational workflow has been improved. If sufficient picks are available in the near range, with an adequate azimuthal coverage, only these picks are used for the location.

We evaluated 3 different GMPEs, all at least partly based on historic Dutch data. The Dost GMPE is based on an attenuation relation that has been shifted using near-range

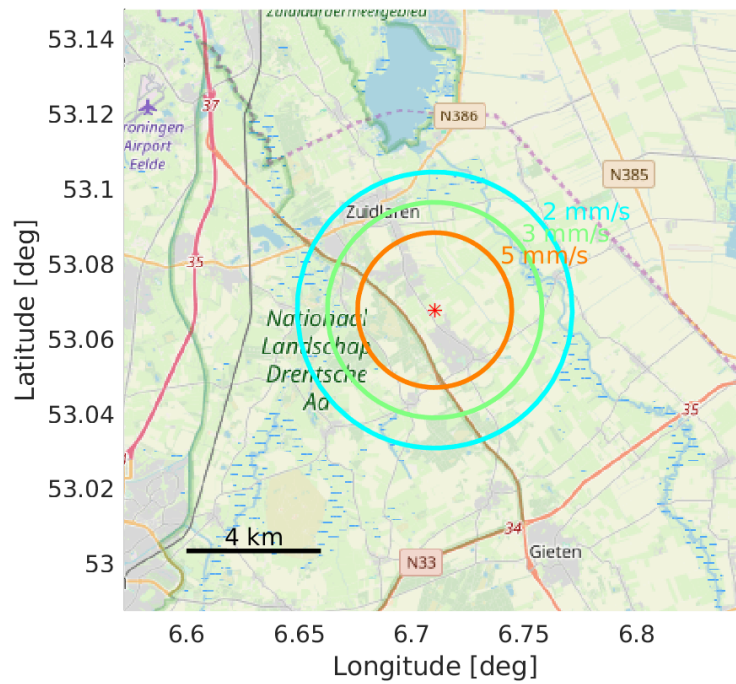


Figure 8: Circles showing the bounding lines of the 2, 3 and 5 mm/s PGV threshold regions for the P90 model, and the updated epicenter (red star).

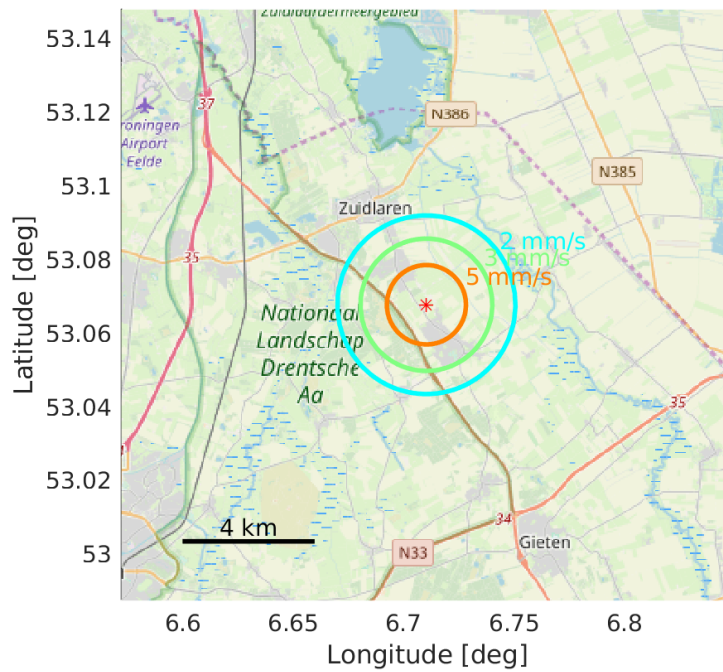


Figure 9: Circles showing the bounding lines of the 2, 3 and 5 mm/s PGV threshold regions for the P50 model, and the updated epicenter (red star).

strong motion recordings. The attenuation beyond 5 km fits well with recent data, but the modest decay in amplitudes over the first 5 km does not fit well with the recent Groningen data. The same holds for the Douglas GMPE which has similarly modest decay over the first 5 km. Moreover, at farther range, Douglas predicts a faster decay in amplitudes than what is observed with recent data. The Bommer GMPE fits best with recent data, which is not surprising since it has been fit using this recent data. The Bommer GMPE has by far the richest empirical base, with a dense sampling of recordings over the first 35 km.

We used the Bommer empirical PGV model and uncertainties derived therein to compute the 99th percentile bound (P99), and also the P90 and P50 bounds. Since many data points were available, the source term could be estimated by shifting the model to fit the data points. Therewith the within-event uncertainty could be eliminated and only the within-earthquake uncertainty was used for defining P99 and P90. Subsequently, we determined the radii R by intersecting P99, P90 and P50 with different PGV threshold values. Final PGV threshold regions were then obtained by drawing circles with radii R with as origin the updated epicenter.

The radii were computed for two definitions of PGV: 1) the geometric mean over the two horizontal components (PGVgeo) and 2) the maximum rotated value (PGVrot). It was shown that the method used for combining the two horizontal components has a large impact on the size of the radii. E.g., the 2 mm/s threshold region for P99 went up from 4.1 to 5.6 km when using PGVrot instead of PGVgeo.

We proposed to use the within-event uncertainty from *Bommer et al. (2019)* also at sites outside of Groningen. This uncertainty is caused, among others, by variation in site condition and azimuthal variation of source radiation. In Groningen, there is a large variation in site conditions, varying from pleistocene sands with little near-surface amplification to medium-deep holocene deposits with large amplification (*Van Ginkel et al., 2019*). Most of the Netherlands is covered with either a pleistocene or pleistocene & holocene blanket. Hence, it is likely that outside of Groningen a similar variability is encountered. Also variability caused by source radiation is likely similar for Groningen and regions outside. Seismicity, both inside and outside Groningen, is characterized by normal faulting on steeply dipping faults.

References

- Bommer, J. J., B. Dost, B. Edwards, P. P. Kruiver, M. Ntinalexis, A. Rodriguez-Marek, P. J. Stafford, and J. van Elk (2017), Developing a model for the prediction of ground motions due to earthquakes in the Groningen gas field, *Netherlands Journal of Geosciences*, *96*(5), s203–s213.
- Bommer, J. J., P. J. Stafford, and M. Ntinalexis (2019), Updated empirical GMPEs for PGV from Groningen earthquakes — March 2019, *NAM*.
- Dost, B., T. Van Eck, and H. Haak (2004), Scaling of peak ground acceleration and peak ground velocity recorded in the Netherlands, *Bollettino di Geofisica Teorica ed Applicata*, *45*(3), 153–168.
- Dost, B., E. Ruigrok, and J. Spetzler (2017), Development of probabilistic seismic hazard assessment for the Groningen gas field, *Netherlands Journal of Geosciences*, *96*(5), s235–s245, doi:10.1017/njg.2017.20.
- Dost, B., B. Edwards, and J. J. Bommer (2018), The relationship between m and m_I : A review and application to induced seismicity in the Groningen gas field, the Netherlands, *Seismological Research Letters*, *89*(3), 1062–1074.

- Douglas, J., B. Edwards, V. Convertito, N. Sharma, A. Tramelli, D. Kraaijpoel, B. M. Cabrera, N. Maercklin, and C. Troise (2013), Predicting ground motion from induced earthquakes in geothermal areas, *Bulletin of the Seismological Society of America*, *103*(3), 1875–1897.
- Jonker, A., C. Ostendorf, and C. Cauberg-Huygen (2017), *SBR Trillingsrichtlijn A: Schade aan bouwwerken:2017*, SBRCURnet, <https://www.naa.nl/wp-content/uploads/2019/04/SBR-Trillingsrichtlijn-A-Schade-aan-bouwwerken-2017.pdf>.
- KNMI (1993), Netherlands Seismic and Acoustic Network, Royal Netherlands Meteorological Institute (KNMI), Other/Seismic Network, doi:10.21944/e970fd34-23b9-3411-b366-e4f72877d2c5.
- Kraaijpoel, D., and B. Dost (2013), Implications of salt-related propagation and mode conversion effects on the analysis of induced seismicity, *Journal of Seismology*, *17*(1), 95–107.
- Kruiver, P. P., et al. (2017), An integrated shear-wave velocity model for the Groningen gas field, the Netherlands, *Bulletin of Earthquake Engineering*, doi: 10.1007/s10518-017-0105-y.
- Lienert, B. R., E. Berg, and L. N. Frazer (1986), HYPOCENTER: An earthquake location method using centered, scaled, and adaptively damped least squares, *Bulletin of the Seismological Society of America*, *76*(3), 771–783.
- report TCBB (2019), Mijnbouwschade, wat nu? Advies landelijke aanpak afhandeling mijnbouwschade en schadeprotocol gaswinning kleine velden op land, *Tech. rep.*, Technische Commissie BodemBeweging, 25-03-2019.
- Spetzler, J., E. Ruigrok, and B. Dost (2018), Improved 3D hypocenter method for induced earthquakes in Groningen, Nederlands Aardwetenschappelijk Congres, March 15-16. Veldhoven, the Netherlands.
- Tarantola, A. (2005), *Inverse Problem Theory and Methods for Model Parameter Estimation*, SIAM, Philadelphia.
- Van Ginkel, J., E. Ruigrok, and R. Herber (2019), Assessing soil amplifications in Groningen, the Netherlands, *First Break*, *37*(10), 33–38.
- Zhou, H.-w. (1994), Rapid three-dimensional hypocentral determination using a master station method, *Journal of Geophysical Research: Solid Earth*, *99*(B8), 15,439–15,455.



Royal Netherlands Meteorological Institute

PO Box 201 | NL-3730 AE De Bilt
Netherlands | www.knmi.nl